Desalination and Water Treatment
www.deswater.com
doi: 10.5004/dwt.2023.29620

302 (2023) 195–209
August

Removal of malachite green from aqueous solution using *Ficus benjamina* activated carbon-metal oxide synthesized by pyrocarbonic acid microwave

Khatab Emad Talib, Sami D. Salman*

Biochemical Engineering Department, Al-Khwarizmi College of Engineering, University of Baghdad, Baghdad 47024, Iraq, email: sami.albayati@gmail.com (S.D. Salman)

Received 29 December 2022; Accepted 15 May 2023

ABSTRACT

Activated carbon has a high adsorption feature because it contains a specific high surface area, as this property helps it to adsorb organic, inorganic, and colloidal substances, whether these substances are liquid or gaseous. In this research, *Ficus benjamina* plant residues were selected as a precursor for preparation of the activated carbon (AC), and composite photocatalyst (AC-TiO_2) adsorbents using pyrocarbonic acid microwave technique. The *Ficus benjamina* and activated carbon was characterized using Fourier-transform infrared spectroscopy, scanning electron microscopy with energy-dispersive X-ray spectroscopy and Brunauer–Emmett–Teller techniques. A certain range of conditions (impregnation time, acid concentration, impregnation ratio, microwave power, and microwave exposure time,) has been identified and analyzed for the production of activated carbon using STATISTICA 12.5 software with Taguchi method. The results showed that the best productivity of activated carbon in a specific range of condition was 80% phosphoric acid concentration, 1:2 impregnation ratio (weight ratio), 6-h impregnation time, 20-min microwave exposure time and 700-watt microwave power. Likewise, Taguchi method was used to identified and analyzed the experimental adsorption data of initial dye concentration, mixing time, and adsorbent dosage. In addition, the adsorption data were analyzed and fitted by Langmuir and Freundlich isotherm models, and the result was well fitted with the Freundlich model. Likewise, the adsorption kinetics were fitted with pseudo-first-order and pseudo-second-order models and the results were well represented by the pseudo-second-order model.

Keywords: *Ficus benjamina* plant; Pyrocarbonic acid; Microwave; Activated carbon; Surface area; Design of experiment

1. Introduction

The adsorption process is used as an efficient physical technique for removing or reducing the concentration of a variety of organic and inorganic pollutants from water effluent [1–5]. The fact that activated carbon (AC) as a renowned adsorbent, may be utilized effectively to remove a wide range of contaminants from the environment. Activated carbon is an amorphous form of carbon that is specially treated to produce a highly developed internal pore structure and a large surface area, thus, producing a reasonably cheap and excellent adsorbent [6]. Activated carbon has highly developed porosity, large surface area (that can reach 3,000 m^2/g), variable characteristics of surface chemistry, and a high degree of surface reactivity so it can be identified as a very effective adsorbent for the removal of a wide variety of organic and inorganic pollutants dissolved in aqueous media [7,8] or from the gaseous environment [9,10]. Currently, around 275,000 tons of AC are consumed annually worldwide [10,11]. Most of the materials used to prepare AC are mineral carbons [11] and lignocellulosic from biomass, wood, and some agricultural wastes [10]. Two methods are used for the production of AC, namely, chemical activation (ChA) (activation with mineral salts) and

* Corresponding author.

physical activation (PhA) (activation using oxidizing agents such as CO_2 or steam). In ChA, the precursor is impregnated with an activating agent such as $ZnCl_2$, H_3PO_4, KOH, H_2SO_4, and NaOH followed by carbonization with conventional heating by an electrical furnace in an inert atmosphere at temperatures ranging from 400°C to 800°C or carbonization with microwave heating [12,13]. Possible advantages of ChA over PhA include higher yield, simplicity (no need for the previous carbonization of raw material), lower temperature of activation, and good development of the porous structure [14]. A variety of methods such as precipitation, adsorption, evaporation, reverse osmosis, and ion-exchange have been employed to remove some pollutants from water or wastewater, among which adsorption with AC is considered to be the best technology for the removal of color, nitrate, chemical oxygen demand and heavy metals except for its high manufacturing cost as said by [15,16]. Coal, wood, and coconut shell are the most widely used carbonaceous materials for the industrial production of ACs as said by [17]. But these types are often expensive and imported which makes it necessary for developing countries to find a cheap and available feedstock for the preparation of AC for use in industry, drinking water purification, and wastewater treatment. Agricultural by-products can be broadly classified into two groups: (a) soft, compressible waste products of low density such as rice husks, sugarcane bagasse, peanut shells, soybean shells, etc. and (b) hard, dense, and not easily compressed agricultural by-products such as pecan or walnut shells, and stones from dates, apricots or cherries. Several suitable agricultural by-products including; olive cakes [17], olive stone [7,18], olive waste cakes [19], dates stone [14,20], tobacco stems [21], almond shells [10,22], corn cob [23], date palm fronds [24] waste tea [25], waste apricot [26], sawdust [27–29], cherry stones [30], rice bran [31], durian shell [32], herb residues [33,34] cotton stalk [13] Siri's seed pods [35,36] have been investigated in the last years as AC precursors and are still receiving renewed attention. A comparison of the malachite green adsorption capacity from aqueous solution using different adsorbents [37–55] is illustrated in Table 1.

The present work was conducted using the *Ficus benjamina* plant used as a precursor for the preparation of the activated carbon (AC), and composite photocatalyst (AC-TiO_2) adsorbents using pyrocarbonic acid microwave technique to adsorbate malachite green dye from aqueous solution. High surface area activated carbon was prepared via H_3PO_4

Table 1
Comparison of the malachite green adsorption capacity using different adsorbents

Adsorbents	Surface area (m^2/g)	Microporosity (%)	Pore width (nm)	Adsorption capacity (mg/g)	pH	References
Hemicellulose-based adsorbent				96.1	6.5	[37]
Magnetic-cyclodextrin-graphene oxide nanocomposites				741	7	[38]
Oxidized mesoporous carbon	334	61	3.9	1,265	6.5	[39]
Reduced graphene oxide	931		3.0	476	6	[40]
Carboxylate group-functionalized multi-walled carbon nanotubes	400		1.5	11.8	9	[41]
Potassium salts-activated carbons from textile sludge	481	57	34	167	6	[42]
Magnetic $CuFe_2O_4$ nano-adsorbent	128		1.8	197	5.4	[43]
Starch-graft poly(acrylamide)/hydrogels				287	5.5	[44]
Sulfonic acid-modified coal fly ash	69.4		3.0	233		[45]
Zeolite nanostructures from waste aluminum cans				227		[46]
Bio-based magnetic activated carbon	389	69	4.6	218	6	[47]
Fibrous cellulose sulfate	36.6			960	6	[48]
Tetraethylenepentamine-functionalized activated carbon				333	8	[49]
Lignin sulfonate-based mesoporous materials	118		3.8	121	7	[50]
Nickel hydroxide nanoplates-modified activated carbon	960	87	3.5	76.9	6.5	[39]
ZnO nanorod-loaded activated carbon				20	6	[52]
Copper nanowires loaded on activated carbon	689		7.4	164	5	[53]
Steam/H_3PO_4-activated carbon produced from waste-printed circuit boards	730	40.2	2.5	769		[54]
Magnetic metal–organic framework composite	35.4			114		[55]
Ficus benjamina activated carbon	951.33		4.2034	395.96	2	Present study

activation by microwave heating. The design of the experiment program was used with the Taguchi method, and five variables with four levels were used to investigate and analyzed the effects of impregnation time, acid concentration, impregnation ratio, microwave power, and microwave exposure time on the activated carbon surface area and yield. Also, five variables with four levels that study the effect of agitation speed, mixing time, pH, the concentration of dye, and dose of adsorbents on the malachite green removal efficiency were investigated and analyzed.

2. Method and design of experiments

2.1. Preparation step of activated carbon

Ficus benjamina waste was collected from the gardens of the University of Baghdad. These wastes include twigs firstly washed with water to remove dirt and dust and dried for 24 h in an oven at 100°C. The dried waste was crushed and sieved to (720 μm–1 mm). The sample was impregnated in different concentrations 50%–80% of H_3PO_4 with different impregnated ratios (1–4) and different impregnation times (2–8). The impregnated samples were filtered to remove excess acid and poured into a glass reactor instilled in a microwave oven with different radiation power 280–700 W and different times of irradiation under nitrogen flow of 150 cc/min [56]. The produced samples of activated carbon were washed with hot water to remove the acid residue until pH reached 6.5–7, then dried at 105°C for 24 h and crushed to desired particle size. The present technique quoted the least expensive production cost of activated carbon with chemical activation using phosphoric acid H_3PO_4 and microwave carbonization with a minimum cost estimated as $0.05/g compared to the cost of other production techniques [57,58] The ranges of the impregnation ratio, impregnation time, acid concentration, radiation power and radiation time as independent variables with their levels are using Taguchi design methodology shown in Table 2. Taguchi method with 16 experiments was generated by STATISTICA 12.5 Software as shown in Table 3.

2.2. Characterization of precursor and adsorbents

The *Ficus benjamina* and activated carbon were characterized using Fourier-transform infrared spectroscopy (FTIR), scanning electron microscopy (SEM) with EDS, and Brunauer–Emmett–Teller (BET) techniques. The specific surface area of AC was determined using the liquid nitrogen adsorption–desorption isotherm. Brunauer–Emmett–Teller (BET: HORIBA, SA-900 Series, USA) was used to calculate the specific surface area.

Table 2
Independent variables and their levels for Taguchi design for activated carbon production

Parameter	Factor	Variable level			
Impregnation ratio (wt./wt.)	X_1	1:1	1:2	1:3	1:4
Impregnation time (h)	X_2	2	4	6	8
Acid concentration (wt.%)	X_3	50	60	70	80
Radiation power (Watt)	X_4	280	420	560	700
Radiation time (min)	X_5	10	20	30	40

2.3. Adsorbate preparation

Malachite green (MG) dye stock at various concentrations was prepared from a standard solution of MG dye by dissolving 1 g of MG dye in 1 L of distilled water. The standard solution was diluted with distilled water to achieve the desired dye solution concentrations 20–80 mg/L. The various concentration of dye was determined using UV-visible spectroscopy (λ = 617 nm) with a calibration curve as illustrated in Fig. 1.

3. Results and discussion

3.1. Design of experiments

A set of experiments was generated using Taguchi method with experimental results obtained for the surface area and yield of activated carbon prepared is illustrated in Table 4.

Activated carbon yield and surface area were recorded from the results of physical experiments using Taguchi method and calculation of yield and surface area after the activation process, respectively. The yield of activated carbon on the other hand was found to range from 49.3432% to 49.6158% whereas, the activated carbon surface ranging from 2.2667 to 951.33 m^2/g. The final empirical formula model for yield (Y_1) and surface area (Y_2) shown in Eqs. (1) and (2), respectively, were fitted with experimental data for yield model R^2 = 0.9482 and R^2 = 0.987314.

$$Y_1 = b_0 + b_1X_1 + b_2X_2 + b_3X_3 + b_4X_4 + b_5X_5 + b_{12}X_1X_2 + b_{13}X_1X_3 + b_{14}X_1X_4 + b_{15}X_1X_5 + b_{11}X_1^2 + b_{22}X_2^2 + b_{33}X_3^2 + b_{44}X_4^2 + b_{55}X_5^2 \quad (1)$$

$$Y_2 = b_0 + b_1X_1 + b_2X_2 + b_3X_3 + b_4X_4 + b_5X_5 + b_{12}X_1X_2 + b_{13}X_1X_3 + b_{14}X_1X_4 + b_{15}X_1X_5 + b_{12345}X_1X_2X_3X_4X_5 + b_{11}b_{11}X_1^2 + b_{22}X_2^2 + b_{33}X_3^2 + b_{44}X_4^2 + b_{55}X_5^2 \quad (2)$$

where Y_1 and Y_2 are activated carbon yield and surface area, b_0, b_1, b_2, b_3, b_4 and b_5 are the linear coefficients, b_{12}, b_{13}, b_{14}, and b_{15}, are the second-order interaction terms, b_{11}, b_{22}, b_{33}, b_{44} and b_{55} are the quadratic terms of each factor. X_1, X_2, X_3, X_4, and X_5 are the coded terms of immersion rate, acid concentration, immersion time, radiation exposure time, and radiation energy, respectively. The estimated values of the model coefficient, the standard error of each model term, and its p-value are shown in Tables 5 and 6. It's clearly noted from these tables, that all coefficients have a significant effect on model accuracy due to their p-values which are smaller than 0.05.

Figs. 2 and 3 represent the actual values vs. the predicted values for surface area and yield, respectively. These figures show that the quadratic model of the responses fit the experimental data, which is reflected in the good predictions of the models. The interaction effect between the models' terms is crucial and could be examined based on the model equation and significant effects. The three-dimensional

Table 3
Taguchi method for experimental design of activated carbon preparation

Number	Impregnation ratio	Acid concentration	Impregnation time	Radiation exposure time	Radiation power
1	1:1	50	2	10	700
2	1:1	60	4	20	560
3	1:1	70	6	30	420
4	1:1	80	8	40	280
5	1:2	50	4	30	280
6	1:2	60	2	40	420
7	1:2	70	8	10	560
8	1:2	80	6	20	700
9	1:3	50	6	40	560
10	1:3	60	8	30	700
11	1:3	70	2	20	280
12	1:3	80	4	10	420
13	1:4	50	8	20	420
14	1:4	60	6	10	280
15	1:4	70	4	40	700
16	1:4	80	2	30	560

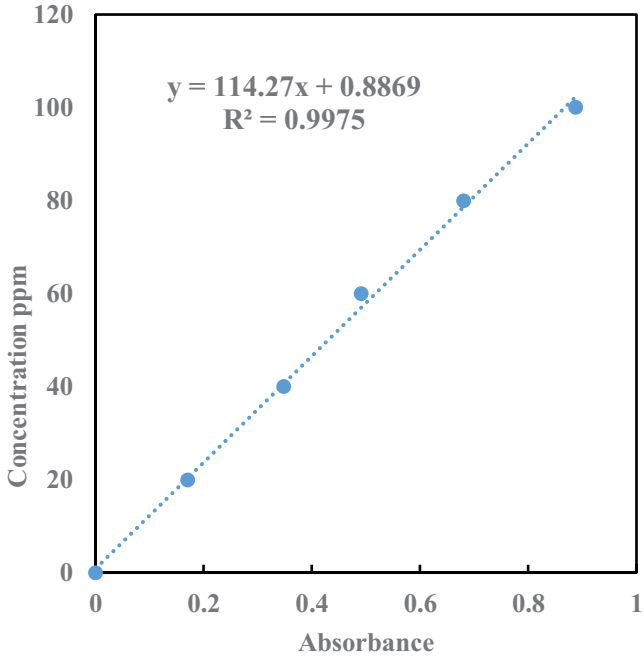

Fig. 1. Calibration curve of malachite green concentration.

surface plot of all the variables is the best way to clearly present the relationships.

In addition, the composite activated carbon was prepared by impregnating 25 g of AC with a high surface area in 250 mL of an aqueous suspension containing 1.25 g of TiO_2 powder. The mixture was heated at 80°C for 5 h with 300 rpm stirring and the product was filtered, and the solid was washed with distilled water until the color in the residual liquid disappeared, then the solid product dried for 24 h at 120°C, to obtain the desired adsorbent for the MG dye removal. SEM and BET analyses were used to undertake a qualitative investigation of AC before adsorption.

3.2. BET analysis for activated carbon

The BET surface areas of activated carbons derived from *Ficus benjamina* were found to be relatively high, with 951.33 m^2/g being the ideal surface area. The pore diameters of sawdust and caw bones were determined to be in the nanopore range on average. The average pore width was calculated to be 4.2034 nm, as shown in Table 7. which conforms to IUPAC nanoporous material categories within the provided range [59].

3.3. Scanning electron microscopy with energy-dispersive X-ray spectroscopy

The surface form and topographical features were investigated using a SEM. The resulting photos are three-dimensional and precisely portray the surface shape. The energy-dispersive X-ray spectrophotometer is used to analyze the elements that make up the precursors energy-dispersive X-ray spectroscopy (EDS). TESCAN, Vega III, Czech Republic, was used for SEM-EDS analysis as shown in Fig. 3a, the best AC produced from 16 runs in run 8 from Table 3. The surface morphology for AC has been developed with lamellar structure with different pores sizes and shapes. These pores' heterogeneity in sizes and shapes have resulted from the breakdown and volatilization of non-carbonaceous material in feedstock and the resulting pores formed due to chemical gives a good probability for dyes to be adsorbed. Whereas Fig. 3b shows the surface morphology of AC-TiO_2 with spongy nature and a large number of cavities, the presence of metal nanoparticles, and layers of carbon particles [59]. Elemental compositions of activated carbons (AC) and composite photocatalysts

Table 4
Experimental design of optimization of production of activated carbon

Number	Impregnation ratio	Acid concentration	Impregnation time	Exposure time	Radiation power	Yield %	BET (m^2/g)
1	1:1	50	2	10	700	49.5334	825.05
2	1:1	60	4	20	560	49.5956	809.12
3	1:1	70	6	30	420	49.6158	585.18
4	1:1	80	8	40	280	49.555	418.21
5	1:2	50	4	30	280	49.3432	13.015
6	1:2	60	2	40	420	49.4864	17.683
7	1:2	70	8	10	560	49.4364	16.615
8	1:2	80	6	20	700	49.5638	951.33
9	1:3	50	6	40	560	49.5288	14.26
10	1:3	60	8	30	700	49.5064	37.268
11	1:3	70	2	20	280	49.4104	2.2667
12	1:3	80	4	10	420	49.506	15.808
13	1:4	50	8	20	420	49.3854	11.274
14	1:4	60	6	10	280	49.3462	10.352
15	1:4	70	4	40	700	49.473	31.942
16	1:4	80	2	30	560	49.53	6.8107

Table 5
Model coefficients, standard error, and terms *p*-values for activated carbon yield

Coefficient	Estimate	Standard error	*t*-value df = 1	*p*-value	Lo. conf. limit	Up. conf. limit
b_0	472.5532	0.080445	39.631748	0.033453476	472.5532	472.5532
b_1	–5.7924	0.722492	–18.434666	0.022354676	–5.7924	–5.7924
b_2	–3.3206	0.022664	–10.55949	0.04876435	–3.3206	–3.3206
b_3	–16.4448	0.000643	–33.050914	0.027356476	–16.4448	–16.4448
b_4	–1.5723	0.000258	–17.919547	0.0176345	–1.5723	–1.5723
b_5	0.2530	0.031082	64.572202	0.0376854	0.2530	0.2530
b_{11}	0.0158	0.023694	21.239910	0.012134253	–0.2852	0.3169
b_{22}	0.0007	0.000257	91.755232	0.028765	–0.0032	0.0033
b_{33}	–0.0020	0.006396	–64.020965	0.043786523	–0.0833	0.0793
b_{44}	–0.0001	0.000261	–148.61886	0.0237564	–0.0034	0.0033
b_{55}	–0.0003	0.018365	–30.472067	0.017564335	–0.0000	–0.0000
b_{12}	0.0328	0.000041	11.996309	0.0376565	0.0328	0.0328
b_{13}	0.1630	0.002099	31.034637	0.02874556	0.1630	0.1630
b_{14}	0.0312	0.000354	27.952689	0.0345378	0.0312	0.0312
b_{15}	–0.0025	0.001782	–8.12495113	0.022764534	–0.0025	–0.0025

(AC-TiO_2) were analyzed by EDS their results are shown in Fig. 4a and b. It's clearly from these figures that carbon percentage for active carbon was 81.19%.

3.4. Fourier-transform infrared spectroscopy

Fourier-transform infrared spectroscopy was utilized to determine the functional groups that occur on the surface of both *Ficus benjamina* and activated carbon. The infrared spectra were examined using a Fourier-transform infrared spectrophotometer (IRAffinity-1 Shimadzu, Japan) as shown in Fig. 5b the best AC was produced from 16 runs in run 8 from Table 4. Fig. 5a shows the FTIR for *Ficus benjamina*.

The FTIR spectra of *Ficus benjamina* and AC are shown in Fig. 4a and b. The FTIR spectra clearly have lower intensities than the *Ficus benjamina* spectrum, and many of the *Ficus benjamina* peaks have vanished. The dissolution of chemical bonds during H_3PO_4 impregnation creates this evanescence, which subsequently leads the carbonization process to remove and liberate a range of volatile compounds [60]. Four peaks were discovered in the AC FTIR spectra at 3,425; 1,647; 1,554 and 1,415 cm^{-1}. The initial peak at 3,425 cm^{-1} was probably induced by the O–H stretching vibration of the hydroxyl groups [61]. The band around 1,647 cm^{-1} might be attributed to C≡C stretching vibrations in alkyne groups, while the peak around 1,554 cm^{-1} could be attributed to C=C stretching vibrations in aromatic rings

Table 6
Model coefficients, standard error, and terms *p*-values for activated carbon surface area

Coefficient	Estimate	Standard error	*t*-value df = 1	*p*-value	Lo. conf. limit	Up. conf. limit
b_0	3,282,444	0.023364	32.9754396	0.012423	1.827109E+39	–1.827109E+39
b_1	–42,604	0.000076	25.7865392	0.00234235	1.809098E+37	–1.809098E+37
b_2	–27,924	0.003078	–11.3465982	0.01433234	2.283770E+37	–2.283770E+37
b_3	–145,450	0.000563	–32.6667493	0.03763458	1.141887E+38	–1.141887E+38
b_4	–14,470	0.000298	–18.9667532	0.04423652	1.141877E+37	–1.141877E+37
b_5	2,152	0.006396	61.7647372	0.03323748	1.631238E+36	–1.631238E+36
b_{11}	100	0.001033	23.3959108	0.01237472	4.299873E+31	–4.299873E+31
b_{22}	0.00754	0.002275	89.5852727	0.02234346	5.453686E+29	–5.453686E+29
b_{33}	–18	0.090664	66.2098652	0.0334525	1.170699E+31	–1.170699E+31
b_{44}	–1	0.000643	–166.618867	0.01463256	4.490555E+29	–4.490555E+29
b_{55}	0.002397	0.000887	–28.721067	0.02134513	3.188241E+27	–3.188241E+27
b_{12}	276	0.003678	18.9896914	0.03451351	2.261162E+35	–2.261162E+35
b_{13}	1,441	0.000161	33.3467375	0.04534134	1.130581E+36	–1.130581E+36
b_{14}	287	0.013835	26.5627685	0.02334534	2.261143E+35	–2.261143E+35
b_{15}	–21	0.000071	8.95771313	0.0116567	1.615088E+34	–1.615088E+34
b_{12345}	0.00075	0.000877	39.6317483	0.0236534	–1.626432E-07	–1.626432E-07

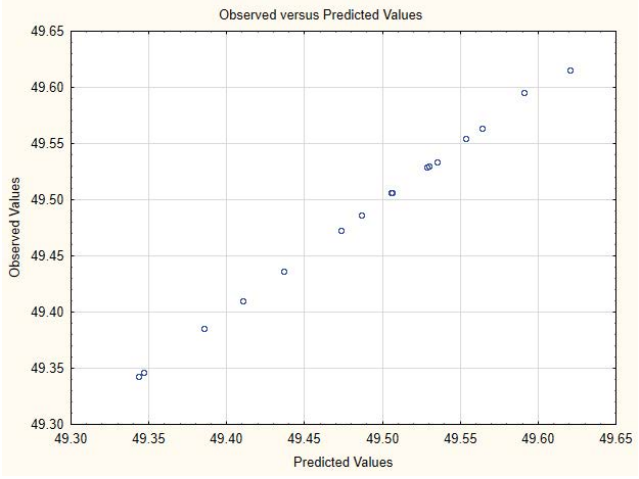

Fig. 2. Comparison between the actual and predicted value for yield.

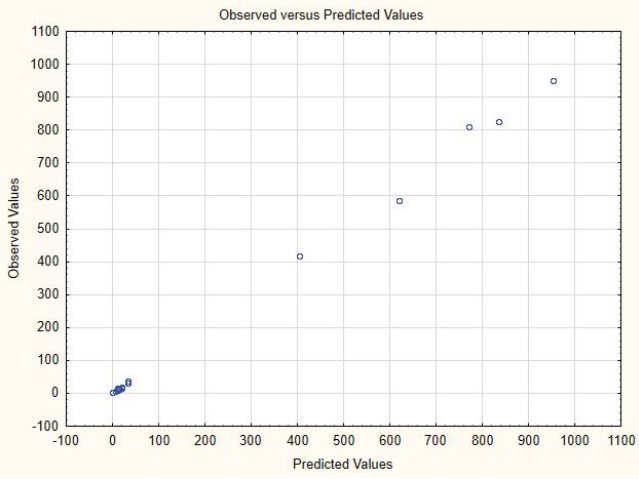

Fig. 3. Comparison between the actual and predicted value for surface area.

[62]. The existence of C–O stretching vibrations in alcohols, phenols, acids, ethers, or esters is indicated by the 1,415 peak [63].

3.5. Batch experimental studies

Batch experiments with five independent factors with four levels of initial dye concentration, mixing time, and adsorbent dosage were selected for design experiments as shown in Table 8, whereas Taguchi method with 16 experiments was generated by STATISTICA 12.5 Software to investigate their impact on the quality of MG dye adsorption as shown in Table 9. was proposed using Taguchi method as described before and the response as experimental removal efficiency illustrated in Table 8. The batch experiments were carried out to evaluate the factors' effects and their interaction on the removal efficiency of MG. 250 mL Erlenmeyer flask containing the necessary adsorbent 0.1–0.4 g/L of AC-TiO_2 and 20–80 ppm of malachite green dye solution. The solution was agitated on a temperature-controlled mixer for a specified contact period 20–100 min. The mixture of AC-TiO_2 and dye solution was filtered after specific time intervals to remove the solid from the solution. Ultraviolet-visible spectroscopy was used to determine the equilibrium concentration of malachite green dye. The MG adsorption capacity and efficiency was determined in Eqs. (3) and (4).

$$q_e = \frac{\left(C_o - C_e\right)V}{M} \tag{3}$$

$$\text{RE\%} = \frac{\left(C_o - C_e\right)}{C_o} \tag{4}$$

where C_o and C_e are dye initial and equilibrium concentrations (ppm), respectively; q_e is the equilibrium capacity of MG (mg/g); V is the volume of malachite green solution (L); M is the mass of AC-TiO_2 (g).

The removal efficiency of malachite green by AC alone was found to range from 98.99% to 91.39%, for the AC-TiO_2 was found to range from 99.13% to 95.39%. This means that the presence of TiO_2 enhanced the adsorption of MG on activated carbon. The empirical formula model for removal efficiency by AC (Y_1) and AC-TiO_2 (Y_2) as illustrated in Eqs. (5) and (6), respectively, were fitted with experimental data for removal model R^2 = 99.455565, and R^2 = 98.914094.

$$Y_1 = b_0 + b_1X_1 + b_2X_2 + b_3X_3 + b_4X_4 + b_5X_5 + b_{12}X_1X_2 + b_{13}X_1X_3 + b_{14}X_1X_4 + b_{15}X_1X_5 + b_{12345}X_1X_2X_3X_4X_5 + b_{11}X_1^2 + b_{22}X_2^2 + b_{44}X_4^2 + b_{55}X_5^2 \quad (5)$$

Table 7
BET analysis for activated carbon

Parameter	Value
Sample weight (g)	0.0416
Standard volume (cm^3)	9.779
Dead volume (cm^3)	15.408
Equilibrium time (s)	0
Adsorptive (N_2)	N_2
Apparatus temperature (C)	0
Adsorption temperature (K)	77.000
Saturated vapor pressure (Kpa)	84.424
Adsorption cross-section area (mm^2)	0.162
BET plot	
V_m (cm^3(STP)/g)	218.57
$a_{s,BET}$ (m^2/g)	951.33
C	312.26
Total pore volume (p/p_0 = 0.990) (cm^3/g)	0.9997
Mean pore diameter (nm)	4.2034

$$Y_2 = b_0 + b_1X_1 + b_2X_2 + b_3X_3 + b_4X_4 + b_5X_5 + b_{12}X_1X_2 + b_{13}X_1X_3 + b_{14}X_1X_4 + b_{15}X_1X_5 + b_{12345}X_1X_2X_3X_4X_5 + b_{11}b_{11}X_1^2 + b_{22}X_2^2 + b_{44}X_4^2 + b_{55}X_5^2 \quad (6)$$

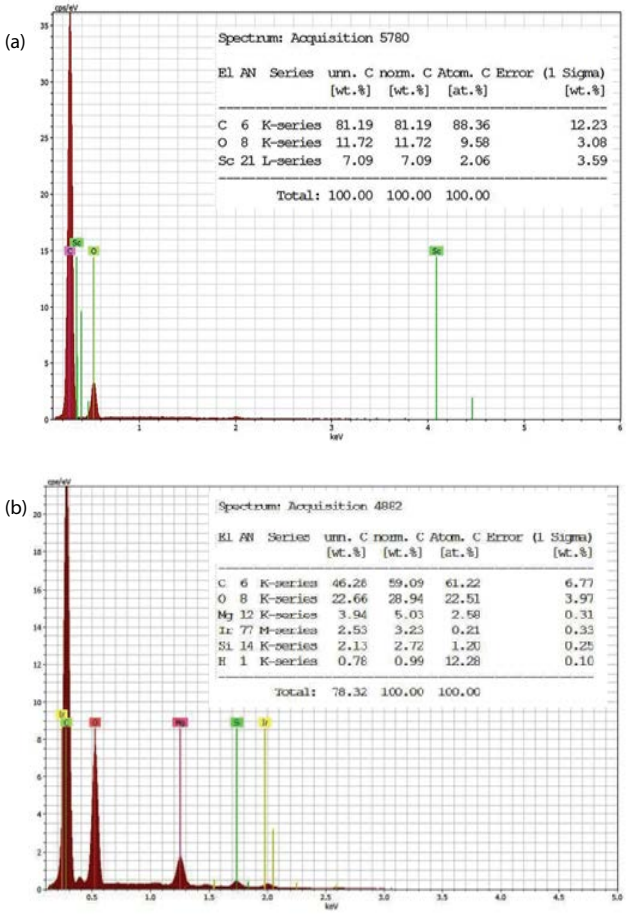

Fig. 4. Energy-dispersive X-ray spectroscopy for (a) activated carbon (b) AC-TiO_2.

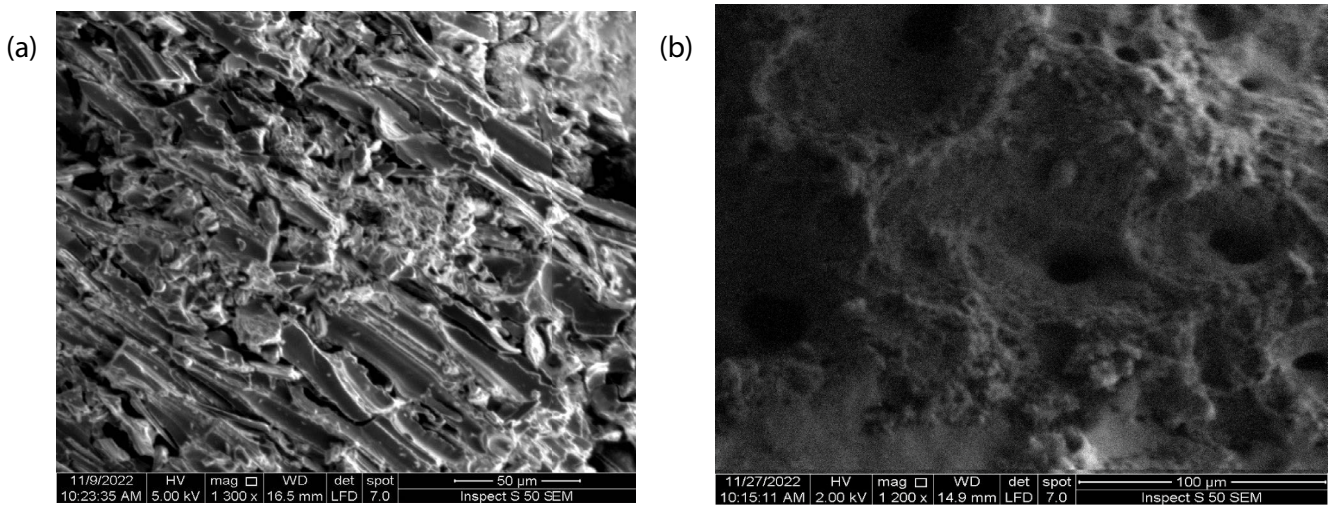

Fig. 3. Scanning electron microscopy for (a) activated carbon and AC-TiO_2.

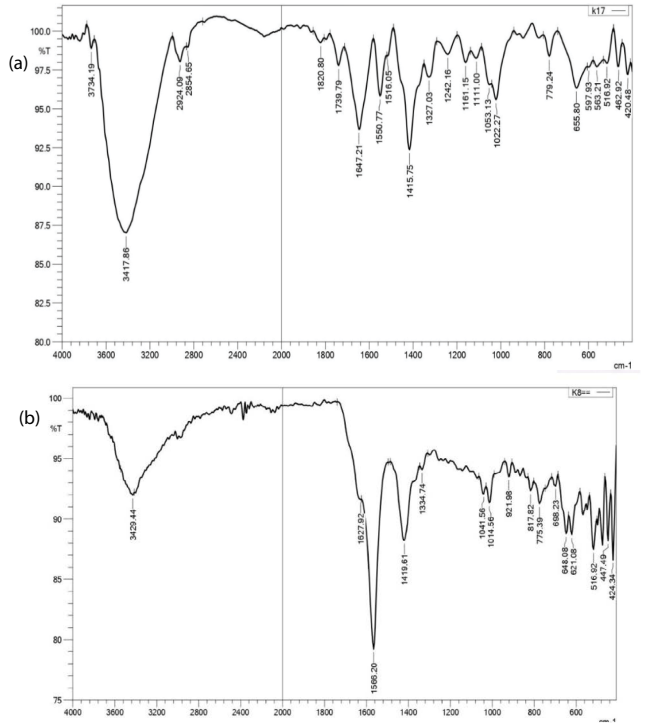

Fig. 5. Fourier-transform infrared spectroscopy for (a) *Ficus benjamina* and (b) activated carbon from run 8.

Table 8
Factors with their levels of Taguchi design method

Parameter	Factor	Level			
Dye concentration (wt.%)	X_1	20	40	60	80
Mixing time (min)	X_2	20	40	60	100
pH	X_3	2	4	6	8
Speed of mixing (rpm)	X_4	200	400	600	800
Dose of activated carbon	X_5	0.10	0.20	0.30	0.40

where Y_1 and Y_2 are removal efficiency for AC alone and AC with TiO_2, b_0, b_1, b_2, b_3, b_4 and b_5 are the linear coefficients, b_{12}, b_{13}, b_{14}, and b_{15}, are the second-order interaction terms, b_{11}, b_{22}, b_{33}, b_{44} and b_{55} are the quadratic terms of each factor. X_1, X_2, X_3, X_4, and X_5 are the coded terms of MG concentration, mixing time, pH, speed of mixing, and dosage of AC, respectively.

The estimated values of the model coefficient, the standard error of each model term, and its *p*-value are shown in Tables 10 and 11. It's clearly noted from these tables, that all coefficients have a significant effect on model accuracy due to their *p*-values which are smaller than 0.05.

3.6. Surface response analysis

Three-dimensional surface plot of the experimental parameter's interaction effects on MG removal efficiency for concentration 20–80 mg/L, mixing time 20–100 min, pH of the solution 2–8, and adsorbent dose 0.1–0.4 g/50 mL of AC and AC-TiO_2 are illustrated in Figs. 6a–d and 7a–d. Figs. 6a and 7a demonstrate the effect of MG concentration and mixing time on removal efficiency for AC and AC-TiO_2, respectively. In general, there are two possible explanations for the cationic dye adsorption mechanism by AC and AC-TiO_2. The first one is due to the electrostatic interaction between the positively charged cationic dyes and the negatively charged of adsorbents and the second one is due to van der Waals interactions between hexagonally arrayed carbon atoms in the graphite sheet of AC and TiO_2 atoms, as well as carbon atoms of the adsorbents and the aromatic backbones of the dyes [64]. It clearly noted that as the initial dye concentration increased, with the mixing time the removal efficiency increased, and the rate of MG adsorption on AC and AC-TiO_2 increased rapidly due to the availability of a great number of unoccupied sites on the surface of the adsorbent, therefore, the dye adsorption rate is high at the beginning. Whereas the colonization of the remaining unoccupied sites becomes more difficult with increasing time due to increased repulsive interactions between dye molecules and bulk solution [65,66]. The obtained results are similar to that obtained by bagasse fly ash and activated carbon [67] and oil palm trunk fiber [68]. Figs. 6b and 7b demonstrate the effect of MG concentration and pH on removal efficiency for AC and AC-TiO_2, respectively. pH of the solution is regarded as the most important element influencing the adsorption capacity is the surface charge intensity of the adsorbent and the ion concentration in the solution [69]. It's clearly noted that the removal efficiency of MG increased as the pH of the solution increased until reach approximately pH 5. This implies that the adsorbent's surface was negatively charged, which allowed more electrostatic attraction for malachite green absorption. similar results were reported for bamboo leaf ash [70], pea shells [71], zinc oxide nanoparticles loaded with activated carbon [72], and wood apple shell [73] adsorbents. Figs. 6c and 7c illustrate the effect of malachite green concentration and agitation speed on removal efficiency for AC and AC-TiO_2,

Table 9
Taguchi method for a batch design experiment

C_i	Time	pH	RPM	Dosage	RE% AC	RE% TiO_2
20	20	2	200	0.1	91.97%	95.39%
20	40	4	400	0.2	95.39%	95.96%
20	60	6	600	0.3	94.82%	96.53%
20	100	8	800	0.4	94.82%	96.53%
40	20	4	600	0.4	97.12%	98.26%
40	40	2	800	0.3	96.55%	97.69%
40	60	8	200	0.2	97.12%	97.98%
40	100	6	400	0.1	96.55%	97.98%
60	20	6	800	0.2	97.89%	98.65%
60	40	8	600	0.1	90.10%	98.27%
60	60	2	400	0.4	98.46%	99.03%
60	100	4	200	0.3	97.89%	98.65%
80	20	8	400	0.3	98.56%	98.85%
80	40	6	200	0.4	98.70%	98.85%
80	60	4	800	0.1	98.99%	98.85%
80	100	2	600	0.2	98.70%	99.13%

Table 10
Model coefficients, standard error, and terms *p*-values for removal malachite green by activated carbon

Coefficient	Estimate	Standard error	*t*-value df = 1	*p*-value	Lo. conf. limit	Up. conf. limit
b_0	–1.20280	1.415525	–18.434666	0.002323	–19.1887	16.78315
b_1	0.10260	0.068950	64.572202	0.012123	–0.7735	0.97870
b_2	–0.00463	0.003633	39.631748	0.005745	–0.0508	0.04153
b_3	0.13595	0.082218	–30.472067	0.045645	–0.9087	1.18063
b_4	0.00165	0.001344	11.996309	0.009764	–0.0154	0.01874
b_5	3.78324	2.268078	–10.55949	0.001256	–25.0354	32.60190
b_{12}	–0.00039	0.000238	–64.020965	0.004564	–0.0034	0.00264
b_{13}	–0.00577	0.003665	–17.919547	0.005837	–0.0523	0.04080
b_{14}	–0.00006	0.000042	27.952689	0.006747	–0.0006	0.00047
b_{15}	–0.10023	0.067252	–148.61886	0.007655	–0.9548	0.75428
b_{12345}	–0.00000	0.000030	91.755232	0.002345	–0.0000	–0.00000
b_{11}	0.00003	0.000010	–8.12495113	0.007897	–0.0001	0.00016
b_{22}	0.00010	0.000060	31.034637	0.007845	–0.0007	0.00087
b_{44}	–0.00000	0.000763	21.239910	0.007845	–0.0000	–0.00000
b_{55}	–3.81895	2.352758	–33.050914	0.001260	–33.7136	26.07567

Table 11
Model coefficients, standard error, and terms *p*-values for removal malachite green by AC-TiO_2

Coefficient	Estimate	Standard error	*t*-value df = 1	*p*-value	Lo. conf. limit	Up. conf. limit
b_0	–1.20280	1.415525	39.631748	0.0321	–19.1887	16.78315
b_1	0.10260	0.068950	–64.020965	0.0281	–0.7735	0.97870
b_2	–0.00463	0.003633	–33.050914	0.0189	–0.0508	0.04153
b_3	0.13595	0.082218	31.034637	0.0213	–0.9087	1.18063
b_4	0.00165	0.001344	11.996309	0.0278	–0.0154	0.01874
b_5	3.78324	2.268078	64.572202	0.0256	–25.0354	32.60190
b_{12}	–0.00039	0.000238	91.755232	0.0298	–0.0034	0.00264
b_{13}	–0.00577	0.003665	–17.919547	0.0254	–0.0523	0.04080
b_{14}	–0.00006	0.000042	27.952689	0.0195	–0.0006	0.00047
b_{15}	–0.10023	0.067252	–148.61886	0.0184	–0.9548	0.75428
b_{12345}	–0.00000	0.000000	21.239910	0.0266	–0.0000	–0.00000
b_{11}	0.00003	0.000010	–8.12495113	0.0243	–0.0001	0.00016
b_{22}	0.00010	0.000060	–30.472067	0.0385	–0.0007	0.00087
b_{44}	–0.00000	0.000000	–10.55949	0.0258	–0.0000	–0.00000
b_{55}	–3.81895	2.352758	–18.434666	0.0147	–33.7136	26.07567

respectively. It can be observed from these figures that the influence of the agitation is minor as compared to the effect of concentration which coincide to the results obtained by apricot stones activated carbon [74]. Finally, the effect of malachite green concentration and adsorbent dose on removal efficiency for AC and AC-TiO_2 are illustrated in Figs. 6d and 7d. It's clearly noted that the effect of malachite green concentration is more significant as compared to the adsorbent dose, which means as the concentration increased there are sufficient free sites on the absorbent still available for malachite green adsorption. Similar results were obtained by activated carbon generated from agricultural waste activated carbon [75] and multi-wall carbon nanotubes [76].

3.7. Adsorption isotherm

To match the results in the adsorption isotherms for malachite green adsorption on AC-TiO_2 were performed under the ideal conditions discovered for each case and with different starting concentrations. At different mixing times, the developed experimental model produced different outcomes. To understand the behavior of adsorbate molecules at a solid–liquid interface, several adsorption models can be used. Langmuir (Langmuir 1916) and Freundlich analyzed adsorption data in their work (Freundlich 1925). The Langmuir model has the following linear form:

$$q_e = \frac{k_L q_m C_e}{1 + k_L C_e} \tag{7}$$

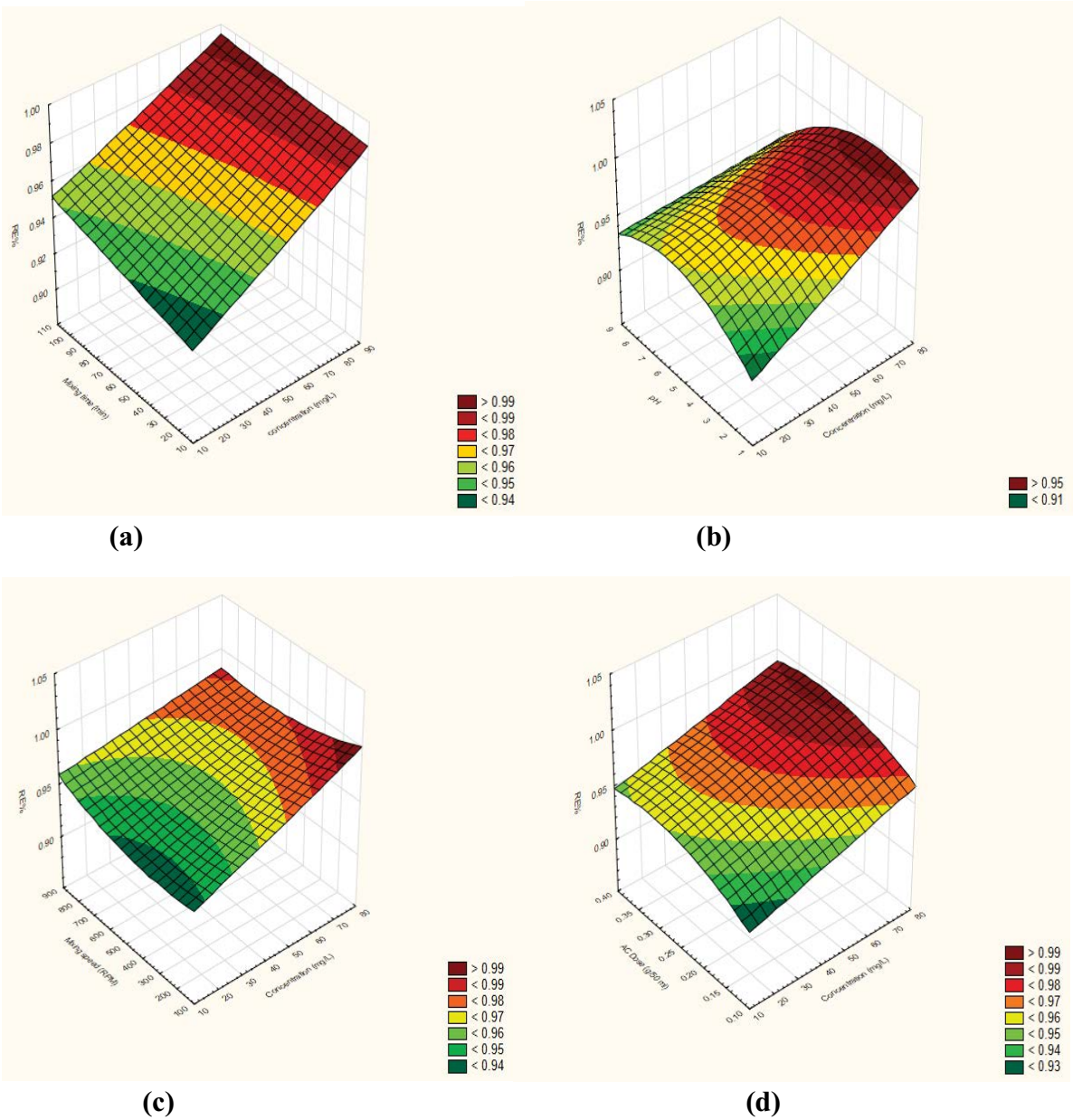

Fig. 6. Effect of (a) malachite green concentration with contact time, (b) malachite green concentration with pH, (c) malachite green concentration with mixing speed and (d) malachite green concentration with activated carbon dose.

where q_e (mg/g) is the equilibrium adsorption capacity, C_e (mg/L) is the equilibrium malachite green concentration, k_L (L/mg) is the adsorption equilibrium constant, and q_m (mg/g) is the complete monolayer adsorption capacity.

The Freundlich isotherm is given in the linear form:

$$q_e = k_f C_e^{1/n} \tag{8}$$

The Freundlich constants k_f (L/mg) and 1/n.

The adsorption behavior of MG on AC and AC-TiO_2 was stated by Langmuir and Freundlich isotherm models as shown in Figs. 8 and 9. It is clearly noted from these figures that the adsorption process data well matched with the Freundlich model which means that the adsorption occurred on the assumption of multilayer adsorption on the heterogeneous surface of AC and AC-TiO_2. This behavior agreed with that reported by [77] and disagreed with results obtained by [60] using different kinds of commercial activated carbon. Table 12 summarizes the Langmuir and Freundlich coefficients that fitted with experimental data for malachite green adsorbed by AC and AC-TiO_2.

3.8. Adsorption kinetics

Experiments with batch MG adsorption on both AC and AC-TiO_2 were carried out to investigate adsorption kinetics under optimal conditions for each concentration and with varied contact times. Other results were obtained from the

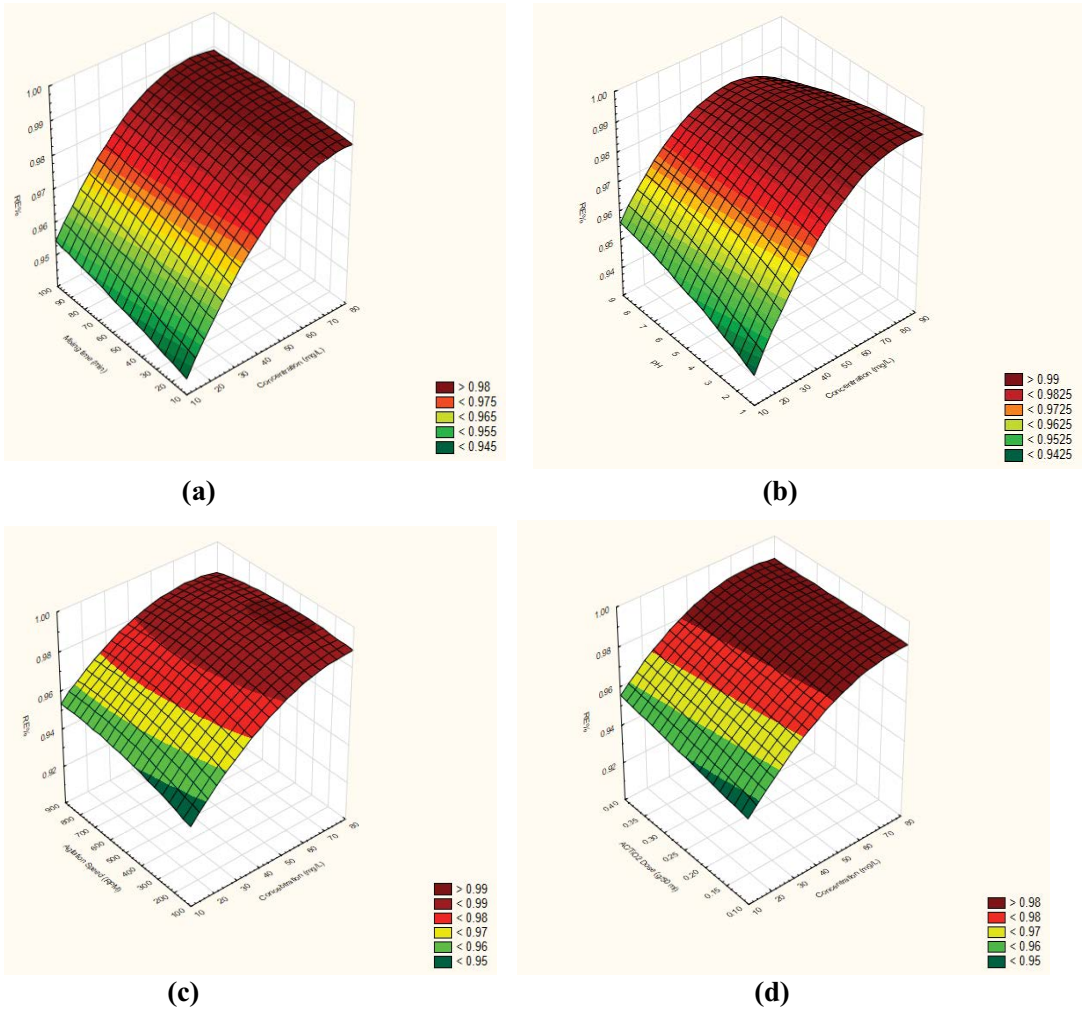

Fig. 7. Effect of (a) malachite green concentration with contact time, (b) malachite green concentration with pH, (c) malachite green concentration with mixing speed and (d) malachite green concentration with AC-TiO_2 dose.

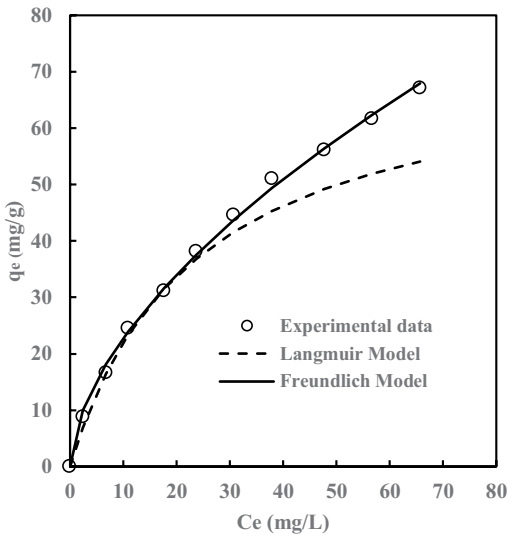

Fig. 8. Langmuir and Freundlich isotherm models for malachite green adsorption by activated carbon.

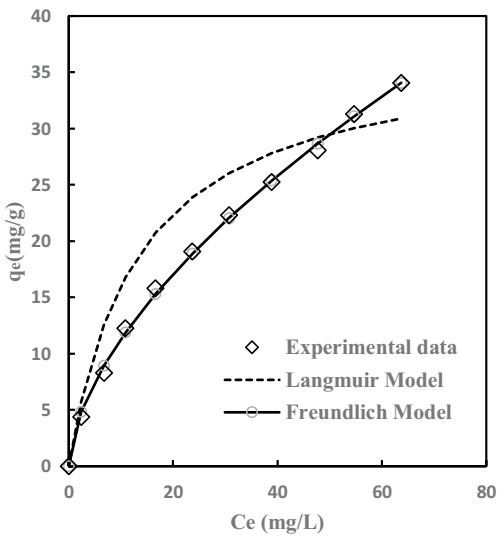

Fig. 9. Langmuir and Freundlich isotherm models for malachite green adsorption by AC-TiO_2.

empirical model when the initial concentrations were varied. Adsorption kinetics defines the interactions between adsorbate and adsorbent, and it is being studied because of its application in the prevention of water pollution. Adsorption kinetics may assess two essential aspects used in the design of adsorption units: response rate and mechanism [78]. The kinetics mechanism was characterized for adsorption data fitting using two models: pseudo-first-order (Lagrange 1906) and pseudo-second-order [78,79]. The pseudo-first-order and pseudo-second-order formulas were used to fit adsorption data as shown in Eqs. (9) and (10):

$$q_t = q_e\left(1 - e^{-k_1 t}\right) \tag{9}$$

$$q_t = \frac{k_2 t q_e^2}{1 + q_e k_2 C_e} \tag{10}$$

where q_e and q_t (mg/g) are the equilibrium adsorption capacities at time t (min), and k_1 (min^{-1}) k_2 (g/mg·min) is the adsorption constants.

Fig. 10 shows the plots of q_t vs. time of adsorption (t) using experimental data compared with pseudo-first-order fitting models for AC whereas Fig. 11 shows the plots of q_t vs. time of adsorption (t) using experimental data with pseudo-first-order models for AC-TiO_2. It's clearly noted that the adsorption process well fitted with a pseudo-second-order model which means that the mechanism of the adsorption process complied with chemisorption. This mechanism was similar to that reported by [42]. The kinetic parameters for the two kinetic models and correlation coefficients are summarized in Table 13.

3.9. Proposed adsorption mechanisms

Various potential interactions, including cationic and ionic exchange, hydrogen bond creation, electrostatic attraction, n–π interaction, π–π interaction, and pore filling have been proposed in the literature for cationic dye adsorption [80], and the adsorption mechanism is greatly related to the structure and properties of the adsorbate [81]. Two processes for the adsorption mechanism of malachite green dye on activated carbon were proposed as illustrated in Fig. 12a and b; monolayer adsorption on the first layer

Table 12
Freundlich and Langmuir coefficients for malachite green adsorption on activated carbon and AC-TiO_2

Adsorbent	Langmuir			Freundlich		
	k_L (L/mg)	q_m (mg/g)	R^2	k_f (mg/g)	n	R^2
Activated carbon	0.0426	73.356	0.958	5.9644	1.7203	0.9993
AC-TiO_2	0.0750	37.356	0.9646	2.8725	1.6798	0.9996

Table 13
Kinetic parameters and correlation coefficients for activated carbon and AC-TiO_2

	Pseudo-first-order			Pseudo-second-order		
	k_1 (min^{-1})	$q_{e,cal}$ (mg/g)	R^2	k_2 (g/mg·min)	$q_{e,cal}$ (mg/g)	R^2
Activated carbon	0.1248	37.4772	0.9388	0.00229	43.9151	0.9995
AC-TiO_2	0.1630	40.7945	0.9412	0.00778	40.8717	0.9911

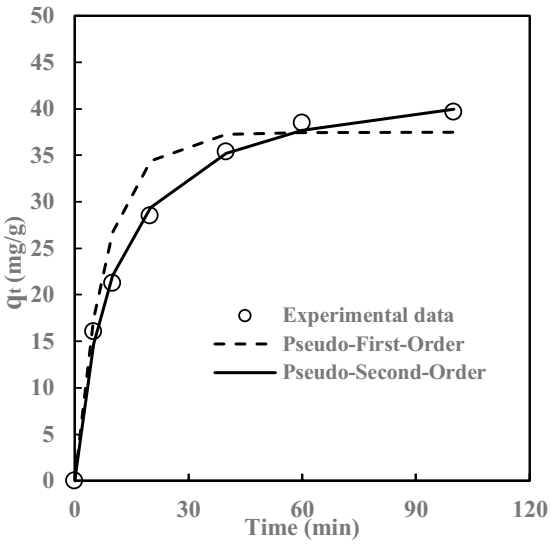

Fig. 10. Plots of pseudo-first-order and pseudo-second-order adsorption kinetics of malachite green on activated carbon.

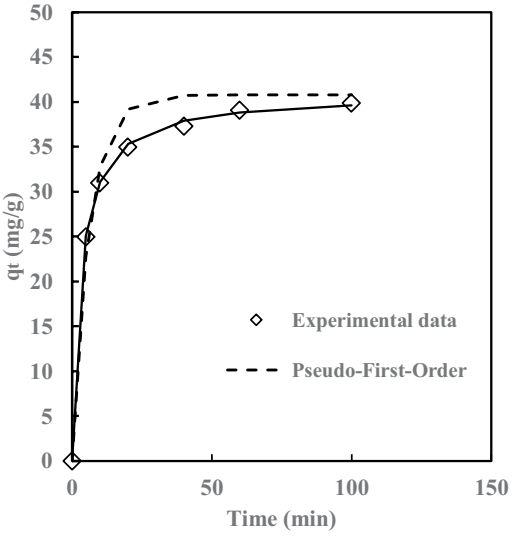

Fig. 11. Plots of pseudo-first-order and pseudo-second-order adsorption kinetics of malachite green on AC-TiO_2.

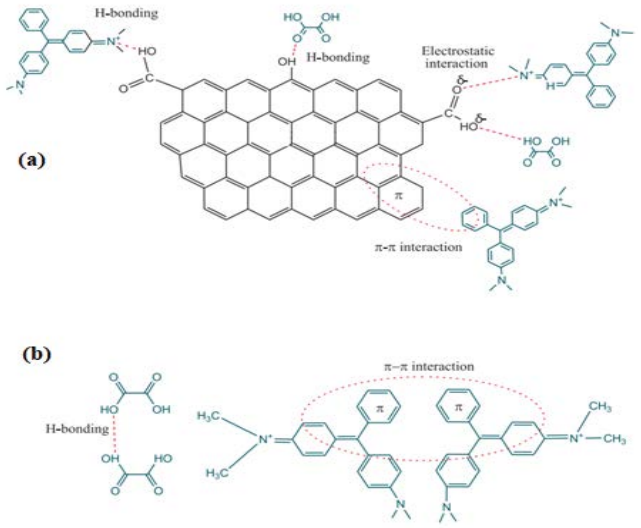

Fig. 12. Adsorption mechanism of (a) malachite green and activated carbon interaction, malachite green molecules interaction.

and multilayer adsorption on the posterior layers (ref). Fig. 11a shows three steps for potential monolayer adsorption interactions, (i) an electrostatic interaction between the carboxylic groups in the adsorbent surface and the cationic charge of the MG dye, (ii) H-bonding between the carboxyl or hydroxyl groups in the adsorbent surface and H-bonding in malachite green as well H-bonding between hydroxyl group in malachite green and carbonyl group in the adsorbent surface, (iii) π–π interaction between aromatic groups in adsorbent surface and malachite green molecules. Whereas, Fig. 11b shows two steps for potential multilayer adsorption interactions (i) π–π interactions between the aromatic rings of the malachite green and, (ii) H-bonding between hydroxyl group in malachite green molecules [82]. In addition, Lewis acidic and basic sites in TiO_2 allow its surface to be easily hydroxylated by dissociation and adsorption of water molecules during the AC-TiO_2 preparation sample. TiO_2 molecules on the surface of the activated carbon are bonded by hydroxyl groups and the slightly increasing of malachite green adsorption is attributed to the electrostatic interactions between the cationic dyes and the metal oxide's negative surface [83].

4. Conclusion

The present research revealed that *Ficus benjamina* agro-waste can effectively be used as a raw material for the preparation of activated carbon by pyrocarbonic acid microwave method with titanium oxide (TiO_2) as composite material for the removal of malachite green dye from aqueous solutions. The experiment conditions with the method of activation were optimized using the experimental design methodology and the results were analyzed with the STATISTICA 12.5 Software. The analyzed results showed that the best removal efficiency of AC adsorbent reached 98.99% at operating conditions of 40 min, pH 4, mixing speed 800 rpm, and 0.1 g/50 mL adsorbent dose. Whereas the best removal efficiency of AC-TiO_2 adsorbent reached 99.13% at operating conditions of 100 min, pH 2, mixing speed 600 rpm, and 0.2 g/50 mL adsorbent dose. In addition, the analysis of the results showed that the adsorption process followed the Freundlich and pseudo-second-order kinetic models which explained that the adsorption may involve multilayer adsorption behavior with interactions between the adsorbate molecules and the availability of the adsorbent sites than the adsorbate concentration pesticides in solution.

Acknowledgements

The authors are grateful to the Biochemical Engineering Department, Al-Khwarizmi College of Engineering, University of Baghdad, for their support to carry out this research work.

References

[1] H. Yang, H. Zhang, Y. Yao, B.Y. Dong, Effect of average refrigerant temperature on freezing-based combined seawater desalination, Desal. Water Treat., 157 (2019) 8–17.
[2] H. Soner Altundoğan, S. Altundoğan, F. Tümen, M. Bildik, Arsenic removal from aqueous solutions by adsorption on red mud, Waste Manage., 20 (2000) 761–767.
[3] T. Guo, H. Yang, Q. Liu, H. Gu, N. Wang, W. Yu, Y. Dai, Adsorptive removal of phosphate from aqueous solutions using different types of red mud, Water Sci. Technol., 2017 (2018) 570–577.
[4] G. Nirmala, T. Murugesan, K. Rambabu, K. Sathiyanarayanan, P.L. Show, Adsorptive removal of phenol using banyan root activated carbon, Chem. Eng. Commun., 208 (2021) 831–842.
[5] A. Patel, S. Soni, J. Mittal, A. Mittal, C. Arora, Sequestration of crystal violet from aqueous solution using ash of black turmeric rhizome, Desal. Water Treat., 220 (2021) 342–352.
[6] Y. Alhamed, Activated carbon from date stone by $ZnCl_2$ activation, J. King Saud Univ. Eng. Sci., 17 (2006) 75–100.
[7] N. Fiol, I. Villaescusa, M. Martínez, N. Miralles, J. Poch, J. Serarols, Sorption of Pb(II), Ni(II), Cu(II) and Cd(II) from aqueous solution by olive stone waste, Sep. Purif. Technol., 50 (2006) 132–140.
[8] O. Ioannidou, A. Zabaniotou, Agricultural residues as precursors for activated carbon production—a review, Renewable Sustainable Energy Rev., 11 (2007) 1966–2005.
[9] J.M. Dias, M.C.M. Alvim-Ferraz, M.F. Almeida, J. Rivera-Utrilla, M. Sánchez-Polo, Waste materials for activated carbon preparation and its use in aqueous-phase treatment: a review, J. Environ. Manage., 85 (2007) 833–846.
[10] J.M.V. Nabais, C.E.C. Laginhas, P.J.M. Carrott, M.M.L. Ribeiro Carrott, Production of activated carbons from almond shell, Fuel Process. Technol., 92 (2011) 234–240.
[11] C.I. Sainz-Diaz, A.J. Griffiths, Activated carbon from solid wastes using a pilot-scale batch flaming pyrolyser, Fuel, 79 (2000) 1863–1871.
[12] H. Deng, L. Yang, G. Tao, J. Dai, Preparation and characterization of activated carbon from cotton stalk by microwave assisted chemical activation—application in methylene blue adsorption from aqueous solution, J. Hazard. Mater., 166 (2009) 1514–1521.
[13] H. Deng, G. Li, H. Yang, J. Tang, J. Tang, Preparation of activated carbons from cotton stalk by microwave assisted KOH and K_2CO_3 activation, Chem. Eng. J., 163 (2010) 373–381.
[14] Y.A. Alhamed, S. Arabia, Activated carbon from dates' stone by $ZnCl_2$ activation, JKAU: Eng. Sci., 17 (2006) 75–100.
[15] M. Ajmal, R.A.K. Rao, M.A. Khan, Adsorption of copper from aqueous solution on *Brassica campestris* (mustard oil cake), J. Hazard. Mater., 122 (2005) 177–183.
[16] H. Demiral, C. Güngör, Adsorption of copper(II) from aqueous solutions on activated carbon prepared from grape bagasse, J. Cleaner Prod., 124 (2016) 103–113.

[17] R. Baccar, J. Bouzid, M. Feki, A. Montiel, Preparation of activated carbon from Tunisian olive-waste cakes and its application for adsorption of heavy metal ions, J. Hazard. Mater., 162 (2009) 1522–1529.
[18] R. Ubago-Pérez, F. Carrasco-Marín, D. Fairén-Jiménez, C. Moreno-Castilla, Granular and monolithic activated carbons from KOH-activation of olive stones, Microporous Mesoporous Mater., 92 (2006) 64–70.
[19] A. Baçaoui, A. Yaacoubi, A. Dahbi, C. Bennouna, R. Phan Tan Luu, F.J. Maldonado-Hodar, J. Rivera-Utrilla, C. Moreno-Castilla, Optimization of conditions for the preparation of activated carbons from olive-waste cakes, Carbon, 39 (2001) 425–432.
[20] N.M. Haimour, S. Emeish, Utilization of date stones for production of activated carbon using phosphoric acid, Waste Manage., 26 (2006) 651–660.
[21] A.-N.A. El-Hendawy, A.J. Alexander, R.J. Andrews, G. Forrest, Effects of activation schemes on porous, surface and thermal properties of activated carbons prepared from cotton stalks, J. Anal. Appl. Pyrolysis, 82 (2008) 272–278.
[22] M.G. Plaza, C. Pevida, C.F. Martín, J. Fermoso, J.J. Pis, F. Rubiera, Developing almond shell-derived activated carbons as CO_2 adsorbents, Sep. Purif. Technol., 71 (2010) 102–106.
[23] Q. Cao, K.-C. Xie, Y.-K. Lv, W.-R. Bao, Process effects on activated carbon with large specific surface area from corn cob, Bioresour. Technol., 97 (2006) 110–115.
[24] N.M. Jabbar, S.D. Salman, I.M. Rashid, Y.S. Mahdi, Removal of an anionic Eosin dye from aqueous solution using modified activated carbon prepared from date palm fronds, Chem. Data Collect., 42 (2022) 100965, doi: 10.1016/j.cdc.2022.100965.
[25] B.M.W.P.K. Amarasinghe, R.A. Williams, Tea waste as a low-cost adsorbent for the removal of Cu and Pb from wastewater, Chem. Eng. J., 132 (2007) 299–309.
[26] S. Erdoğan, Y. Önal, C. Akmil-Başar, S. Bilmez-Erdemoğlu, Ç. Sarıcı-Özdemir, E. Köseoğlu, G. İçduygu, Optimization of nickel adsorption from aqueous solution by using activated carbon prepared from waste apricot by chemical activation, Appl. Surf. Sci., 252 (2005) 1324–1331.
[27] H. Zhang, Y. Yan, L. Yang, Preparation of activated carbon from sawdust by zinc chloride activation, Adsorption, 16 (2010) 161–166.
[28] M.W. Khalid, S.D. Salman, Adsorption of heavy metals from aqueous solution onto sawdust activated carbon, Al-Khawarizmi Eng. J., 15 (2019) 60–69.
[29] I.K. Shakir, Kinetic and isotherm modeling of adsorption of dyes onto sawdust, Iraqi J. Chem. Pet. Eng., 11 (2010) 15–27.
[30] C.J. Durán-Valle, M. Gómez-Corzo, V. Gómez-Serrano, J. Pastor-Villegas, M.L. Rojas-Cervantes, Preparation of charcoal from cherry stones, Appl. Surf. Sci., 252 (2006) 5957–5960.
[31] R.M. Suzuki, A.D. Andrade, J.C. Sousa, M.C. Rollemberg, Preparation and characterization of activated carbon from rice bran, Bioresour. Technol., 98 (2007) 1985–1991.
[32] T.C. Chandra, M.M. Mirna, J. Sunarso, Y. Sudaryanto, S. Ismadji, Activated carbon from durian shell: preparation and characterization, J. Taiwan Inst. Chem. Eng., 40 (2009) 457–462.
[33] J. Yang, K.-q. Qiu, Preparation of activated carbons by $ZnCl_2$ activation from herb residues under vacuum, Carbon, 51 (2013) 437, doi: 10.1016/j.carbon.2012.08.039.
[34] M.S. Salman, Removal of sulfate from wastewater by activated carbon, Al-Khawarizmi Eng. J., 5 (2009) 72–76.
[35] M.J. Ahmed, S.K. Theydan, Microporous activated carbon from Siris seed pods by microwave-induced KOH activation for metronidazole adsorption, J. Anal. Appl. Pyrolysis, 99 (2013) 101–109.
[36] M.J. Ahmed, S.K. Theydan, Microwave assisted preparation of microporous activated carbon from Siris seed pods for adsorption of metronidazole antibiotic, Chem. Eng. J., 214 (2013) 310–318.
[37] D. Gautam, S. Kumari, B. Ram, G.S. Chauhan, K. Chauhan, A new hemicellulose-based adsorbent for malachite green, J. Environ. Chem. Eng., 6 (2018) 3889–3897.
[38] D. Wang, L. Liu, X. Jiang, J. Yu, X. Chen, Adsorption and removal of malachite green from aqueous solution using magnetic β-cyclodextrin-graphene oxide nanocomposites as adsorbents, Colloids Surf., A, 466 (2015) 166–173.
[39] X. Zhang, Q. Lin, S. Luo, K. Ruan, K. Peng, Preparation of novel oxidized mesoporous carbon with excellent adsorption performance for removal of malachite green and lead ion, Appl. Surf. Sci., 442 (2018) 322–331.
[40] K. Gupta, O.P. Khatri, Reduced graphene oxide as an effective adsorbent for removal of malachite green dye: plausible adsorption pathways, J. Colloid Interface Sci., 501 (2017) 11–21.
[41] M. Rajabi, B. Mirza, K. Mahanpoor, M. Mirjalili, F. Najafi, O. Moradi, H. Sadegh, R. Shahryari-ghoshekandi, M. Asif, I. Tyagi, S. Agarwal, V.K. Gupta, Adsorption of malachite green from aqueous solution by carboxylate group functionalized multi-walled carbon nanotubes: determination of equilibrium and kinetics parameters, J. Ind. Eng. Chem., 34 (2016) 130–138.
[42] S.H. Tang, M.A.A. Zaini, Malachite green adsorption by potassium salts-activated carbons derived from textile sludge: equilibrium, kinetics and thermodynamics studies, Asia-Pac. J. Chem. Eng., 12 (2017) 159–172.
[43] B.R. Vergis, R. Hari Krishna, N. Kottam, B.M. Nagabhushana, R. Sharath, B. Darukaprasad, Removal of malachite green from aqueous solution by magnetic $CuFe_2O_4$ nano-adsorbent synthesized by one pot solution combustion method, J. Nanostruct. Chem., 8 (2018) 1–12.
[44] H. Hosseinzadeh, S. Ramin, Fabrication of starch-graft-poly(acrylamide)/graphene oxide/hydroxyapatite nanocomposite hydrogel adsorbent for removal of malachite green dye from aqueous solution, Int. J. Biol. Macromol., 106 (2018) 101–115.
[45] S. Dash, H. Chaudhuri, R. Gupta, U.G. Nair, Adsorption study of modified coal fly ash with sulfonic acid as a potential adsorbent for the removal of toxic reactive dyes from aqueous solution: kinetics and thermodynamics, J. Environ. Chem. Eng., 6 (2018) 5897–5905.
[46] E.A. Abdelrahman, Synthesis of zeolite nanostructures from waste aluminum cans for efficient removal of malachite green dye from aqueous media, J. Mol. Liq., 253 (2018) 72–82.
[47] E. Altintig, M. Onaran, A. Sarı, H. Altundag, M. Tuzen, Preparation, characterization and evaluation of bio-based magnetic activated carbon for effective adsorption of malachite green from aqueous solution, Mater. Chem. Phys., 220 (2018) 313–321.
[48] M. Baghdadi, B. Alipour Soltani, M. Nourani, Malachite green removal from aqueous solutions using fibrous cellulose sulfate prepared from medical cotton waste: comprehensive batch and column studies, J. Ind. Eng. Chem., 55 (2017) 128–139.
[49] M. Ghasemi, S. Mashhadi, M. Asif, I. Tyagi, S. Agarwal, V.K. Gupta, Microwave-assisted synthesis of tetraethylenepentamine functionalized activated carbon with high adsorption capacity for malachite green dye, J. Mol. Liq., 213 (2016) 317–325.
[50] Y. Tang, Y. Zeng, T. Hu, Q. Zhou, Y. Peng, Preparation of lignin sulfonate-based mesoporous materials for adsorbing malachite green from aqueous solution, J. Environ. Chem. Eng., 4 (2016) 2900–2910.
[51] F. Nekouei, H. Kargarzadeh, S. Nekouei, I. Tyagi, S. Agarwal, V. Kumar Gupta, Preparation of nickel hydroxide nanoplates modified activated carbon for malachite green removal from solutions: kinetic, thermodynamic, isotherm and antibacterial studies, Process Saf. Environ. Prot., 102 (2016) 85–97.
[52] M. Ghaedi, F. Azad, K. Dashtian, S. Hajati, A. Goudarzi, M. Soylak, Central composite design and genetic algorithm applied for the optimization of ultrasonic-assisted removal of malachite green by ZnO nanorod-loaded activated carbon, Spectrochim. Acta, Part A, 167 (2016) 157–164.
[53] M. Ghaedi, E. Shojaeipour, A.M. Ghaedi, R. Sahraei, Isotherm and kinetics study of malachite green adsorption onto copper nanowires loaded on activated carbon: artificial neural network modeling and genetic algorithm optimization, Spectrochim. Acta, Part A, 142 (2015) 135–149.

[54] Y. Kan, Q. Yue, J. Kong, B. Gao, Q. Li, The application of activated carbon produced from waste printed circuit boards (PCBs) by H_3PO_4 and steam activation for the removal of malachite green, Chem. Eng. J., 260 (2015) 541–549.
[55] Z. Shi, C. Xu, H. Guan, L. Li, L. Fan, Y. Wang, L. Liu, Q. Meng, R. Zhang, Magnetic metal organic frameworks (MOFs) composite for removal of lead and malachite green in wastewater, Colloids Surf., A, 539 (2018) 382–390.
[56] S.D. Salman, I.M. Rasheed, M.M. Ismaeel, Removal of diclofenac from aqueous solution on apricot seeds activated carbon synthesized by pyrocarbonic acid microwave, Chem. Data Collect., 43 (2023) 100982, doi: 10.1016/j.cdc.2022.100982.
[57] J. Lai, L. Ngu, Comparative laboratory cost analysis of various activated carbon activation process, IOP Conf. Ser.: Mater. Sci. Eng., 1195 (2021) 012018, doi: 10.1088/1757-899X/1195/1/012018.
[58] S. Soni, P.K. Bajpai, D. Bharti, J. Mittal, C. Arora, Removal of crystal violet from aqueous solution using iron-based metal organic framework, Desal. Water Treat., 205 (2020) 386–399.
[59] C. Parvathiraja, S. Katheria, M.R. Siddiqui, S.M. Wabaidur, M.A. Islam, W.-C. Lai, Activated carbon-loaded titanium dioxide nanoparticles and their photocatalytic and anti-bacterial investigations, Catalysts, 12 (2022) 834, doi: 10.3390/catal12080834.
[60] W. Qu, T. Yuan, G. Yin, S. Xu, Q. Zhang, H. Su, Effect of properties of activated carbon on malachite green adsorption, Fuel, 249 (2019) 45–53.
[61] B.H. Hameed, J.M. Salman, A.L. Ahmad, Adsorption isotherm and kinetic modeling of 2,4-D pesticide on activated carbon derived from date stones, J. Hazard. Mater., 163 (2009) 121–126.
[62] J. Yang, K. Qiu, Development of high surface area mesoporous activated carbons from herb residues, Chem. Eng. J., 167 (2011) 148–154.
[63] W. Tongpoothorn, M. Sriuttha, P. Homchan, S. Chanthai, C. Ruangviriyachai, Preparation of activated carbon derived from *Jatropha curcas* fruit shell by simple thermo-chemical activation and characterization of their physico-chemical properties, Chem. Eng. Res. Des., 89 (2011) 335–340.
[64] J.-L. Gong, B. Wang, G.-M. Zeng, C.-P. Yang, C.-G. Niu, Q.-Y. Niu, W.-J. Zhou, Y. Liang, Removal of cationic dyes from aqueous solution using magnetic multi-wall carbon nanotube nanocomposite as adsorbent, J. Hazard. Mater., 164 (2009) 1517–1522.
[65] P. Luo, Y. Zhao, B. Zhang, J. Liu, Y. Yang, J. Liu, Study on the adsorption of neutral red from aqueous solution onto halloysite nanotubes, Water Res., 44 (2010) 1489–97.
[66] M. Mohamed, S.K. Ouki, Kinetic and removal mechanisms of ethylbenzene from contaminated solutions by chitin and chitosan, Water Air Soil Pollut., 220 (2011) 131–140.
[67] I.D. Mall, V.C. Srivastava, N.K. Agarwal, I.M. Mishra, Adsorptive removal of malachite green dye from aqueous solution by bagasse fly ash and activated carbon-kinetic study and equilibrium isotherm analyses, Colloids Surf., A, 264 (2005) 17–28.
[68] B.H. Hameed, M.I. El-Khaiary, Batch removal of malachite green from aqueous solutions by adsorption on oil palm trunk fibre: equilibrium isotherms and kinetic studies, J. Hazard. Mater., 154 (2008) 237–244.
[69] B. Heibati, S. Rodriguez-Couto, M.A. Al-Ghouti, M. Asif, I. Tyagi, S. Agarwal, V.K. Gupta, Kinetics and thermodynamics of enhanced adsorption of the dye AR 18 using activated carbons prepared from walnut and poplar woods, J. Mol. Liq., 208 (2015) 99–105.
[70] Kuntari, D.A. Priwidyanjati, Adsorption of malachite green dye from aqueous solution on the bamboo leaf ash, AIP Conf. Proc., 1911 (2017) 020011, doi: 10.1063/1.5016004.
[71] T.A. Khan, R. Rahman, P.I. Ali, E.A. Khan, A. Mukhlif, Removal of malachite green from aqueous solution using waste pea shells as low-cost adsorbent – adsorption isotherms and dynamics, Toxicol. Environ. Chem., 96 (2014) 569–578.
[72] E. Altıntıg, M. Yenigun, A. Sarı, H. Altundag, M. Tuzen, T.A. Saleh, Facile synthesis of zinc oxide nanoparticles loaded activated carbon as an eco-friendly adsorbent for ultra-removal of malachite green from water, Environ. Technol. Innovation, 21 (2021) 101305, doi: 10.1016/j.eti.2020.101305.
[73] A.S. Sartape, A.M. Mandhare, V.V. Jadhav, P.D. Raut, M.A. Anuse, S.S. Kolekar, Removal of malachite green dye from aqueous solution with adsorption technique using *Limonia acidissima* (wood apple) shell as low-cost adsorbent, Environ. Technol. Innovation, 10 (2017) S3229–S3238.
[74] M. Abbas, Experimental investigation of activated carbon prepared from apricot stones material (ASM) adsorbent for removal of malachite green (MG) from aqueous solution, Adsorpt. Sci. Technol., 38 (2020), doi: 10.1177/0263617420904476.
[75] S. Senthilkumaar, P. Kalaamani, K. Porkodi, P.R. Varadarajan, C.V. Subburaam, Adsorption of dissolved reactive red dye from aqueous phase onto activated carbon prepared from agricultural waste, Bioresour. Technol., 97 (2006) 1618–1625.
[76] C.-H. Wu, Adsorption of reactive dye onto carbon nanotubes: equilibrium, kinetics and thermodynamics, J. Hazard. Mater., 144 (2007) 93–100.
[77] I.A. Rahman, B. Saad, S. Shaidan, E.S. Sya Rizal, Adsorption characteristics of malachite green on activated carbon derived from rice husks produced by chemical–thermal process, Bioresour. Technol., 96 (2005) 1578–1583.
[78] Y.-S. Ho, Citation review of Lagergren kinetic rate equation on adsorption reaction, Scientometrics, 59 (2004) 171–177.
[79] H.P. Boehm, Some aspects of the surface chemistry of carbon blacks and other carbons, Carbon, 32 (1994) 759–769.
[80] H. Tran, Y.-F. Wang, S.-J. You, H.-P. Chao, Insights into the mechanism of cationic dye adsorption on activated charcoal: the importance of π–π interactions, Process Saf. Environ. Prot., 107 (2017) 168–180.
[81] L. Zhang, H. Zhang, W. Guo, Y. Tian, Removal of malachite green and crystal violet cationic dyes from aqueous solution using activated sintering process red mud, Appl. Clay Sci., 93–94 (2014) 85–93.
[82] A.A. Ahmad, M.A. Ahmad, N.K.E.M. Yahaya, J. Karim, Adsorption of malachite green by activated carbon derived from gasified *Hevea brasiliensis* root, Arabian J. Chem., 14 (2021) 103104, doi: 10.1016/j.arabjc.2021.103104.
[83] Z.M. Abou-Gamra, M.A. Ahmed, TiO_2 nanoparticles for removal of malachite green dye from wastewater, Adv. Chem. Eng., 5 (2015) 373–388.